

**PL-TR-97-2060**

# **MAGNETOSPHERIC DYNAMICS: A COMPREHENSIVE STUDY**

**Dennis E. Delorey  
M. Patricia Hagan**

**Boston College  
Institute for Scientific Research  
140 Commonwealth Avenue  
Chestnut Hill, MA 02167**

**31 March 1997**

**Scientific Report No. 1**

**Approved for public release; distribution unlimited**

**DTIC QUALITY INSPECTED 3**



**PHILLIPS LABORATORY  
Directorate of Geophysics  
AIR FORCE MATERIEL COMMAND  
HANSCOM AIR FORCE BASE, MA 01731-3010**

**19970624 146**

This technical report has been reviewed and is approved for publication.



IRVING MICHAEL

Contract Manager

Solar and Interplanetary Effects Branch

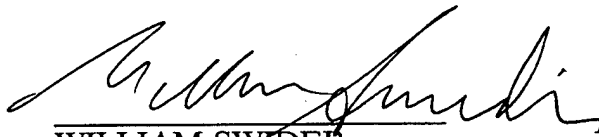
Space Effects Division



MARK D. CONFER, Major, USAF, Chief

Solar and Interplanetary Effects Branch

Space Effects Division



WILLIAM SWIDER

Deputy Director

Space Effects Division

This report has been reviewed by the ESC Public Affairs Office (PA) and is releasable to the National Technical Information Service (NTIS).

Qualified requestors may obtain additional copies from the Defense Technical Information Center (DTIC). All others should apply to the National Technical Information Service (NTIS).

If your address has changed, or if you wish to be removed from the mailing list, or if the addressee is no longer employed by your organization, please notify PL/IM, Hanscom AFB, MA 01731-3010. This will assist us in maintaining a current mailing list.

Do not return copies of this report unless contractual obligations or notices on a specific document require that it be returned.

REPORT DOCUMENTATION PAGE			Form Approved OMB No. 0704-0188	
Public reporting burden for this collection of information is estimated to average 1 hour per response, including the time for reviewing instructions, searching existing data sources, gathering and maintaining the data needed, and completing and reviewing the collection of information. Send comments regarding this burden estimate or any other aspect of this collection of information, including suggestions for reducing this burden, to Washington Headquarters Services, Directorate for Information Operations and Reports, 1215 Jefferson Davis Highway, Suite 1204, Arlington, VA 22202-4302, and to the Office of Management and Budget, Paperwork Reduction Project (0704-0188), Washington, DC 20503.				
1. AGENCY USE ONLY (Leave blank)	2. REPORT DATE 31 March 1997	3. REPORT TYPE AND DATES COVERED Scientific No. 1		
4. TITLE AND SUBTITLE MAGNETOSPHERIC DYNAMICS: A COMPREHENSIVE STUDY		5. FUNDING NUMBERS PE 63707F PR 7601 TA GA WU CB		
6. AUTHOR(S) Dennis E. Delorey and M. Patricia Hagan		Contract: F19628-96-C-0030		
7. PERFORMING ORGANIZATION NAME(S) AND ADDRESS(ES) Boston College Institute for Scientific Research 140 Commonwealth Avenue Chestnut Hill, MA 02167-3862		8. PERFORMING ORGANIZATION REPORT NUMBER		
9. SPONSORING/MONITORING AGENCY NAME(S) AND ADDRESS(ES) Phillips Laboratory 29 Randolph Road Hanscom AFB, MA 01731-3010 Contract Manager: Irving I. Michael/GPSG		10. SPONSORING/MONITORING AGENCY REPORT NUMBER  PL-TR-97-2060		
11. SUPPLEMENTARY NOTES				
12a. DISTRIBUTION / AVAILABILITY STATEMENT  Approved for public release; distribution unlimited			12b. DISTRIBUTION CODE	
13. ABSTRACT (Maximum 200 words)  This report is comprised of thirty-three abstracts of papers presented or published in the first 12-month period of this contract. They are selected as being of the highest scientific interest of all such presentations or publications occurring under this contract during the year.				
14. SUBJECT TERMS Heliospheric imaging, TSS CME, OEDIPUS C, Whistler waves, PL-GEOSpace, Magnetic storms, MSM, SMEI, CRRES, Magnetic clouds, HELIOS			15. NUMBER OF PAGES 20	
			16. PRICE CODE	
17. SECURITY CLASSIFICATION OF REPORT UNCLASSIFIED	18. SECURITY CLASSIFICATION OF THIS PAGE UNCLASSIFIED	19. SECURITY CLASSIFICATION OF ABSTRACT UNCLASSIFIED	20. LIMITATION OF ABSTRACT SAR	



## **Titles of Abstracts of Presentations/Publications Comprising This Scientific Report**

Effects of Ion Environment Variations on the Shuttle Potential During the TSS Missions

Effects of Electron Beam Emissions on the Shuttle Potential During the TSS Missions

Low Frequency Electron Modulations Observed During DC Electron Beam Emissions in the Deployed Phase of TSS-1

Negative Shuttle Charging During TSS 1R

Shuttle Environment During the Prolonged FPEG Beam Emissions of TSS 1R

Shuttle Environment During the Prolonged EGA Beam Emissions of TSS 1R

Low Frequency Electron and Ion Modulations During Electron Beam Emissions in the TSS 1R Deployed Phase

Observations of Electron Heating During the OEDIPUS C Sounding Rocket Experiment

Relationships Between MHz Modulations of Electron Beams Detected During TSS 1R and Whistler Waves Observed During Spacelab 2

Electron Acceleration and Trapping During the OEDIPUS C Sounding Rocket Experiment

Auroral Particle Response to Changing Solar Wind Conditions During the October 1995 Magnetic Cloud Passage

Changes in Density and Temperature of Cusp, Boundary Layer and Polar Rain Populations During the Passage of the October 1995 Magnetic Cloud

Ion Poleward Boundaries and Convection Reversals During the 18-20 October 1995 Magnetic Cloud Passage

Solar Cell Degradation Observed by the Advanced Photovoltaic and Electronics Experiments (APEX) Satellite

PL-GEOSpace: Time Dependent Three-Dimensional Visualization of the Space Environment

A Multi-Satellite View of Energetic Electron Flux Increases at  $L=4-7$  Associated with High Speed Solar Wind Streams

An Observational Test of the Hilmer-Voigt Magnetic Field Model at Geosynchronous Orbit

Requirements for Energetic Electron Flux Enhancements Near  $L = 4.2$ : Relative Geosynchronous Phase Space Density and Geomagnetic Activity

A Magnetospheric Neutral Sheet-Oriented Coordinate System for MSM and MSFM Applications

Modeling Convection Effects in Magnetic Storms

**DTIC QUALITY INSPECTED 3**

Calculated Radiation Belt Electron Lifetimes Compared to CRRES Observations  
CRRES Observations and Radial Diffusion Theory of Radiation Belt Protons  
Comparison of CME Mass and Kinetic Energies Near the Sun and in the Inner Heliosphere  
CMEs as Solar Drivers of Interplanetary and Terrestrial Disturbances  
Geomagnetic Storms and Heliospheric CMEs as Viewed from HELIOS  
CMES and Their Relation to Other Disturbances  
Large-Scale Structures and Multiple Neutral Lines Associated with Coronal Mass Ejections  
The Solar Mass Ejection Imager  
X-ray Signatures of CMEs Observed in White Light  
Heliospheric Imaging Using the Helios Photometers and Thomson Scattering Techniques  
Coronal Mass Ejections and Metric Type II Bursts  
CMEs and Prominences and Their Evolution Over the Solar Cycle (Invited)  
Sudden Disappearances of Polar Crown Filaments as Sources of High Latitude CMEs

**ABSTRACTS FOR:  
PERIOD:**

**Contract F19628-96-C-0030  
February 1996 - March 1997**

*Presentations at the Special Session on Tethers in Space and Results of the TSS 1R Mission at the 1996 Spring Meeting of the American Geophysical Union in Baltimore MD, 20-24 May 1996:*

**Effects of Ion Environment Variations on the Shuttle Potential during the TSS Missions**

L.C. Gentile and C.Y. Huang (Boston College, Institute for Scientific Research, Newton MA 02159)

W.J. Burke, D.A. Hardy and D.G. Olson (PL/GPSG, Hanscom AFB MA 01731)

M.R. Oberhardt (Amptek Inc., Bedford MA 01730)

We present measurements taken by the Shuttle Potential and Return Electron Experiment (SPREE) in the shuttle payload bay during the deployed satellite phases of the Tethered Satellite System (TSS) missions. We study intervals in which the tether was electrically connected to the shuttle by low to medium impedance shunts and thruster firings occurred. For the TSS 1 events the shuttle was flying in an inverse airplane mode with the engine bells facing the ram direction to facilitate ion current collection. The satellite was deployed to 256 m. Ion spectra measured by SPREE indicate that with no thrusters firing the shuttle charged to a few tens of volts negative. In previously reported examples of neutral gas releases from charged spacecraft the magnitude of the vehicle potential decreased. Thruster firings during the TSS 1 events either left the circuit unchanged or caused the current measured in the tether to diminish and the shuttle to become more negatively charged. In the latter case, thruster gas impeded access of ambient ions to the current collecting surfaces of the shuttle. During the longer tether deployment of TSS 1R we anticipate that stronger shuttle potentials will result in occasional breakdowns of ejected neutral gas and subsequent reductions of the shuttle potential.

**Effects of Electron Beam Emissions on the Shuttle Potential during the TSS Missions**

W.J. Burke, D.A. Hardy and D.G. Olson (PL/GPSG, Hanscom AFB MA 01731)

L.C. Gentile and C.Y. Huang (Boston College, Institute for Scientific Research, Newton MA 02159)

M.R. Oberhardt (Amptek Inc., Bedford MA 01730)

We present data acquired by the Shuttle Potential and Return Electron Experiment (SPREE) in the payload bay during the deployed-satellite phases of the Tethered Satellite System (TSS) missions. We study intervals when the tether was electrically connected to the shuttle and dc electron beams were emitted from the Fast Pulsed Electron Generator (FPEG) or the DCORE electron generator assemblies (EGAs). FPEG emits a 100 mA electron beam at an energy of 1 keV. The EGAs are 7.2  $\mu$  pery diodes whose anodes and cathodes are tied to the shuttle ground and the tether potential, respectively. For the studied events the shuttle flew in an inverse airplane mode with the engine bells facing the ram direction to facilitate ion current collection. During TSS-1, with the satellite deployed to 256 m, we observed (1) shuttle charging to several tens of volts positive when FPEG

operated under night conditions, (2) electrons returning to SPREE with energies up to 70 eV while the EGAs fired, and (3) large fluxes of secondary and heated electrons during FPEG but not DCORE emissions. With the tether deployed to 20 km during TSS-1R, the motional emf is approximately 5 kV. This allows the EGAs to emit higher currents, which create many energetic secondary electrons near the shuttle. SPREE monitored the fraction of electrons that returns to the shuttle and their effects on its potential relative to the ambient plasma.

### **Low Frequency Electron Modulations Observed during DC Electron Beam Emissions in the Deployed Phase of TSS-1**

C.Y. Huang and L.C. Gentile (Boston College, Institute for Scientific Research, Newton MA 02159)

D.A. Hardy and W.J. Burke (PL/GPSG, Hanscom AFB MA 01731)

W.J. Raitt and D.C. Thompson (Center for Atmospheric and Space Science, Utah State University, Logan UT 84322)

M.P. Gough (Dept. of Engineering, University of Sussex, Sussex, U.K.)

The Shuttle Potential and Return Electron Experiment (SPREE) was one of the instruments flown in the shuttle payload bay during the TSS 1 mission. The SPREE data processor contains a particle correlator that measures modulations in the electron flux in both kHz and MHz ranges produced by coherent wave-particle interactions. The SPREE was located near the Fast Pulsed Electron gun (FPEG). On 5 August 1992 during the interval from 17:04:50 to 17:07:09 UT, with the tethered satellite deployed to a distance of 224 m, the FPEG emitted a DC beam. During this DC firing, SPREE measured intense fluxes of electrons with densities of approximately  $1.4 \times 10^4$  electron  $\text{cm}^{-3}$ . At energies below 100 eV the flux was nearly isotropic. At higher energies, the flux peaked at pitch angles between 600 and 700 and the electron spectra displayed a thermal shape with a fitted temperature of approximately 100 eV. For pitch angles near 900 the spectra peaked at several hundred eV. During the interval strong modulations of the electron flux were measured by the correlator over a wide range in energy. The electrons in certain energy ranges were observed to be modulated simultaneously at several frequencies. Typically the modulation frequencies were near 300, 1200 and 2500 Hz. They are interpreted as resulting from electron interactions with current-driven, ion acoustic-like waves comparable to those detected during Spacelab 2 [Feng et al., JGR, 97, 17005, 1992].

*Presentations at the Special Session on Results of TSS 1R and the Physics of Charge Collection in Space at the 1996 Fall Meeting of the American Geophysical Union, 15-19 December 1996 in San Francisco CA:*

### **Negative Shuttle Charging during TSS 1R**

L.C. Gentile and C.Y. Huang (Boston College, Institute for Scientific Research, Newton MA 02159-1164)

W.J. Burke, J.S. Machuzak, D.A. Hardy, and D.G. Olson (PL/GPSG, Hanscom AFB MA 01731-3010)

B.E. Gilchrist (University of Michigan, Space Physics Research Laboratory, Ann Arbor MI 48109-2143)

C. Bonifazi (Agenzia Spaziale Italiana, Viale Regina Margherita 202, 00198 Roma, Italia)



Negative shuttle charging events measured by the Shuttle Potential and Return Electron Experiment (SPREE) during the deployed phase of the TSS 1R mission confirm findings from TSS 1 and provide further insights into shuttle-environment effects on the TSS circuit. We have studied 26 intervals when either a 15 ohm or 25k ohm resistor was in the circuit connecting the tether to the shuttle ground and no electron beam emissions occurred. While the tether was deployed, the shuttle flew with its engine bells in the ram direction to facilitate ion current collection from the ionosphere. In the early stages of the deployment with the 15 ohm shunt in the circuit, the shuttle potential decreased monotonically with tether length,  $L$ , from -17 V at 180 m to -245 V at 2560 m. For  $L > 3$  km, only  $\geq 25k$  ohm resistors were used. With no thruster firings, the largest shuttle potential measured with the 25k ohm resistor in the circuit was  $\sim -300$  V near 03:00 LT in a low-density ionosphere at a tether length of  $\sim 5.1$  km. Near local noon with the tether extended to 17.2 km, SPREE measured a potential of -81 V, indicating that ionospheric densities affect the current collecting ability of the shuttle. With the tether deployed to 13.7 km and the 25k ohm resistor in the circuit, the shuttle charged to  $\sim -600$  V. As on TSS 1, we find that firings of the downward pointing vernier thrusters significantly increased the magnitude of the shuttle potential. TSS 1R data also suggest that the residual effects of these firings increased by at least a factor of 3 the time required for the shuttle to return to plasma potential after the circuit was opened.

### **Shuttle Environment during the Prolonged FPEG Beam Emissions of TSS 1R**

W.J. Burke, D.A. Hardy and D.G. Olson (PL/GPSG, Hanscom AFB MA 01731)  
 L.C. Gentile and C.Y. Huang (Boston College, Institute for Scientific Research, Newton MA 02159)  
 W.J. Raitt and D.C. Thompson (Center for Atmospheric and Space Science, Utah State University, Logan UT 84322)  
 B.E. Gilchrist (University of Michigan, Space Physics Research Laboratory, Ann Arbor MI 48109)  
 C. Bonifazi (Agenzia Spaziale Italiana, Viale Regina Margherita 202, 00198 Roma, Italia)

There were thirteen prolonged electron beam emissions from the Fast Pulsed Electron Generator (FPEG) during the deployed phase of TSS 1R. FPEG emitted a 100 mA electron beam at an energy of 1 keV. Environmental responses measured by the Shuttle Potential and Return Electron Experiment (SPREE) during these beam emissions are presented. The shuttle flew in an inverse airplane mode with the engine bells facing the ram direction to facilitate ion current collection. As the tether lengthened from 0.18 to 2.5 km, FPEG fired eight times while a 15 ohm resistor connected the tether to shuttle ground. The potential induced across the system increased from 24 to 210 V. The current flowing through the tether and 15 ohm shunt was systematically higher by a factor of 1.7 when FPEG was firing than when it was not. Unlike the TSS 1 mission, SPREE detected no returning secondary electrons during six consecutive FPEG firing sequences while the shuttle was in sunlight. Most FPEG firings left the shuttle uncharged within  $\pm 10$  V. In one case the shuttle charged positively to a few tens of volts as it crossed an equatorial ionospheric plasma depletion near the dusk terminator. In only one instance did the shuttle charge to significant negative values during an FPEG operation. At that time the tether length was about 15 km and a 25k ohm resistor connected the tether to shuttle ground. The different characteristics of the TSS 1R circuit during FPEG emissions are discussed.

## **Shuttle Environment during the Prolonged EGA Beam Emissions of TSS 1R**

D.G. Olson, W.J. Burke, and D.A. Hardy (PL/GPSG, Hanscom AFB MA 01731)

L.C. Gentile and C.Y. Huang (Boston College, Institute for Scientific Research, Newton MA 02159)

C. Bonifazi (Agenzia Spaziale Italiana, Viale Regina Magherita 202, 00198 Roma, Italia)

B.E. Gilchrist (University of Michigan, Space Physics Research Laboratory, Ann Arbor MI 48109-2143)

We present data acquired in the shuttle payload bay by the Shuttle Potential and Return Electron Experiment (SPREE) during the deployed-satellite phase of the Tethered Satellite System reflight (TSS 1R). We have studied the six prolonged electron beam emissions from the Electron Generator Assemblies (EGAs). The EGAs are 6.4 mP diodes whose anodes and cathodes are tied to the shuttle ground and the tether, respectively. The shuttle flew in an inverse airplane mode with the engine bells facing the ram direction to facilitate ion current collection. During EGA operations, the shuttle was isolated from the tether circuit and its potential floated with respect to the plasma to levels that depended on the flux of beam-generated electrons returning to the shuttle. The prolonged EGA firings occurred with the tether deployed to distances between 6.2 and 16.1 km. The EGAs operated nominally, emitting electron beams with energies and currents up to 1.65 keV and 0.4 A, respectively. We show that: (1) the EGAs utilized more than half the potential generated by TSS, (2) beam electrons created a warm electron cloud that charged the shuttle to as much as -90 V, (3) sheath ionization around the shuttle after thruster firings did not reduce the shuttle potential, and (4) density gradients near the dusk terminator strongly affected the distribution of potential in the TSS circuit.

## **Low Frequency Electron and Ion Modulations during Electron Beam Emissions in the TSS 1R Deployed Phase**

C.Y. Huang and L.C. Gentile (Boston College, Institute for Scientific Research, Newton MA 02159)

D.A. Hardy and W.J. Burke (PL/GPSG, Hanscom AFB MA 01731)

M.P. Gough (Dept. of Engineering, University of Sussex, Sussex, U.K.)

W.J. Raitt and D.C. Thompson (Center for Atmospheric and Space Science, Utah State University, Logan UT 84322)

C. Bonifazi (Agenzia Spaziale Italiana, Viale Regina Magherita 202, 00198 Roma, Italia)

The Shuttle Potential and Return Electron Experiment (SPREE) was flown in the shuttle payload bay during the TSS 1R mission. The SPREE data processor contains a particle correlator that measures modulations in the electron and ion fluxes in both kHz and MHz ranges produced by coherent wave-particle interactions. SPREE was located near two electron-beam emitters, the Fast Pulsed Electron Generator (FPEG) and the Electron Generator Assembly (EGA). While FPEG is confined to emitting a 100 mA beam of electrons with energies of about 1 keV, the EGA is a 6.4 mP diode whose cathode and anode connect to the tether and shuttle ground, respectively. In the DC operations of the EGA the electron beams ranged from 97 mA at 620 eV to 445 mA at 1650 eV.

Between 23:15 UT on February 26 and 00:09 UT on February 27, 1996 while the tether was being deployed there were a number of prolonged electron beam emissions from both FPEG and the EGA during which the fluxes of returning electrons and ions were modulated at frequencies ranging from a few hundred Hz to 5 kHz. On the average, we find that the electron modulation frequencies are lower than those observed previously during the TSS 1 mission. Modulations of ions at frequencies near 600 Hz were regularly detected whenever EGA or FPEG beam emissions resulted in shuttle charging to potentials < -30 V.

## **Observation of Electron Heating During the OEDIPUS C Sounding Rocket Experiment**

David A. Hardy, David G. Olson, William J. Burke, Gregory P. Ginet (AF Phillips Laboratory, Hanscom AFB MA 01731)  
M. Paul Gough (University of Sussex, Sussex, U.K.)  
Cheryl Huang (Boston College, Institute for Scientific Research, Newton MA)  
Robert F. Benson (NASA/GSFC, Greenbelt MD)  
H. Gordon James (Communication Research Centre, Ottawa, Canada)

The OEDIPUS C sounding rocket was launched from the Poker Flat rocket range on Julian day 311, 1995 at 06:38:17 UT. OEDIPUS C was a tethered mother-son payload with a 50 kHz to 8.0 Mhz stepped frequency transmitter on the forward payload and an HF receiver on the aft payload. In the course of the upleg of the flight the tether was deployed to a distance of approximately 1 km. At apogee the tether was cut. As part of the complement of environmental sensors, multiangular electrostatic analyzers were flown on both the forward and aft payloads. These detectors compiled electron spectra over the energy range from 20 eV to 20 keV over a detection fan of 1440 by 100. The HF transmitter was normally swept through 165 frequency steps every 0.5 seconds. The stepping of the electrostatic analyzer was synchronized to the stepping of the transmitter such that the analyzer measured a fixed frequency at each energy step. The output pulses of the electrostatic analyzers were also processed by an onboard particle correlator that measured bunching in the electron flux produced by coherent wave-particle interactions and the time delay between the initiation of waves by the transmitter and the observation of enhanced fluxes in the particle detectors. Throughout the flight the analyzer in the forward payload measured large increases in the electron flux at energies up to several keV whenever the transmitter was emitting at approximately the local electron gyrofrequency, fce. Similar effects were seen on the aft payload for separation up to several hundred meters. At low altitude, weak electron acceleration responses were detected during emissions both below the fce and at its harmonics. The correlator measured clear Mhz modulation of the electrons at the harmonics of the gyrofrequency. Significant time delays were measured between the initiation of the waves and the observations of particle enhancements in the aft payload detector.

*Abstracts submitted for the URSI Meeting in Montreal in July 1997, for the Special Session on Artificial Waves in Space:*

## **Relationships between MHz Modulations of Electron Beams Detected during TSS 1R and Whistler Waves Observed during Spacelab 2**

Cheryl Y. Huang<sup>1</sup>, William J. Burke<sup>2</sup>, M. Paul Gough<sup>3</sup>, Louise C. Gentile<sup>1</sup>, David A. Hardy<sup>2</sup>, and David G. Olson<sup>2</sup>

Systematic experiments were conducted during the latter part of the Tethered Satellite System Reflight (TSS 1R) in which a 1 keV, 100 mA electron beam was emitted from the shuttle for extended intervals at pitch angles near 90°. Rapid plasma responses to these emissions were measured within the beam flux tube by the Shuttle Potential and Return Electron Experiment (SPREE). The SPREE particle correlator identified the energies/angles of time-modulated electron fluxes. Observed modulations at megahertz frequencies fall into two classes: (1) narrow bands that are close in frequency to harmonics of the electron gyrofrequency fce and (2) broad bands that are at interharmonic frequencies. In the latter case, electrons with different energies were modulated at different frequencies.

Whenever SPREE intercepted beam electrons they were found to be modulated at harmonic or interharmonic frequencies after a single gyroturn. These data suggest that beam electrons were modulated by strong beam-plasma interactions very near to the emission aperture. They in turn generated the time-varying electric fields that modulated lower-energy electrons within or near the beam cylinder. During the Spacelab 2 mission, intense whistler waves were detected when the University of Iowa's Plasma Diagnostic Package flew close to the field lines along which electron beams were emitted from the shuttle. Observed whistler intensities and dispersions were consistent with requirements of coherent Cerenkov radiation sources, suggesting that the beam was modulated close to its emission aperture. The detection of modulated beam electrons by SPREE provides strong experimental confirmation of this hypothesis.

<sup>1</sup>Boston College, Institute for Scientific Research, Chestnut Hill MA

<sup>2</sup>USAF Phillips Laboratory, Hanscom AFB MA

<sup>3</sup>University of Sussex, Sussex, UK

### **Electron Acceleration and Trapping during the OEDIPUS C Sounding Rocket Experiment**

William J. Burke<sup>1</sup>, David A. Hardy<sup>1</sup>, M. Paul Gough<sup>2</sup>, Cheryl Y. Huang<sup>3</sup>, Louise C. Gentile<sup>3</sup>, and David G. Olson<sup>1</sup>

The OEDIPUS C sounding rocket was launched from the Poker Flat rocket range on November 7, 1995 at 0638:17 UT. OEDIPUS C was a tethered mother-son payload with a 50 kHz to 8.0 MHz stepped frequency transmitter on the forward payload and an HF receiver on the aft payload. In the course of the upleg of the flight, the tether was deployed to a distance of ~1.2 km. At apogee the tether was cut. As part of the complement of environmental sensors, multiangular electrostatic analyzers (ESAs) were flown on both the forward and aft payloads. These detectors compiled electron spectra from 20 eV to 20 keV in energy over a detection fan of 140° by 8°. The HF transmitter normally swept through 165 frequency steps every 0.5 seconds. During each 3 ms step, the transmitter was turned on for only the first 300 ms. The stepping of the ESA was synchronized with the transmitter so that the analyzer sampled all electron energies at each frequency step. The output pulses of the ESAs were also processed by an onboard particle correlator to detect bunching of electron fluxes produced by coherent wave-particle interactions and time delays between the initiation of waves by the transmitter and the observation of enhanced fluxes by the ESAs.

Throughout the flight the analyzer in the forward payload measured large increases in the electron flux at energies up to several keV whenever the transmitter was emitting at approximately the local electron gyrofrequency  $f_{ce}$ . Similar effects were observed on the aft payload for separations up to several hundred meters. At low altitudes, weak electron acceleration responses were detected in association with emissions both below  $f_{ce}$  and at its harmonics. The correlator measured clear MHz modulations of accelerated electrons at the harmonics of the  $f_{ce}$ , indicating strong particle trapping of accelerated electrons by the emitted waves. There were significant time delays between the initiation of wave transmissions and the detection of particle enhancements by the aft payload ESA. This presentation relates ESA observations to the theory of electron cyclotron interactions and discusses potential applications of wave emission technologies in the magnetosphere.

<sup>1</sup>USAF Phillips Laboratory, Hanscom AFB MA

<sup>2</sup>University of Sussex, Sussex, UK

<sup>3</sup>Boston College, Institute for Scientific Research, Chestnut Hill MA

**Auroral Particle Response to Changing Solar Wind Conditions during the October 1995 Magnetic Cloud Passage**

F. Rich<sup>1</sup>, M.S. Gussenhoven<sup>1</sup>, D. Hardy<sup>1</sup>, and C. Huang<sup>2</sup>

Three DMSP satellites, two in the noon-midnight and one in a dawn-dusk configuration, were in-flight during the October 18-20 magnetic storm period. A shock initiating the magnetic activity was followed by the passage of a magnetic cloud in which the solar wind magnetic field direction and density varied slowly and systematically while the solar wind speed and magnetic field magnitude were near constant. The data from the DMSP satellites afford an opportunity to investigate changes in auroral precipitation and the cross polar cap potential associated with the slow changes within the magnetic cloud and to compare them with those predicted by magnetohydrodynamic simulations of the magnetosphere under similar conditions. Of particular interest are a) the changing position and width of the dayside cusp; b) the intensity, extent and uniformity of particle precipitation in the nightside auroral oval; c) the response time of the magnetosphere to solar wind variations; d) the precise relationship between  $B_z$  and  $B_y$  in triggering polar cap activity and convection pattern changes; e) the relationship of the cross-cap potential to  $B_z$  and magnetospheric activity. Of particular interest is whether the magnetosphere responds in an instability-triggered or a steady manner to  $B_z$  slowly increasing from large negative values to large positive values.

<sup>1</sup>USAF Phillips Laboratory, Hanscom AFB MA

<sup>2</sup>Boston College, Institute for Scientific Research, Chestnut Hill MA

**Changes in Density and Temperature of Cusp, Boundary Layer and Polar Rain Populations during the Passage of the October 1995 Magnetic Cloud**

M.S. Gussenhoven<sup>1</sup>, F. Rich<sup>1</sup>, D. Hardy<sup>1</sup>, and C. Huang<sup>2</sup>

Three distinct populations in the magnetosphere are believed to result from near-direct entry of solar wind particles: 1) the cusp population near noon; 2) the boundary populations at high latitudes on the flanks of the magnetosphere; and 3) the polar rain. The position and extent of these populations have been shown to vary strongly with  $B_z$  and in some cases, solar wind speed, IMF sector, magnetic activity and season. Direct comparison of the three populations with each other and with the assumed parent population are rare, and somewhat troubling in their differences. A variety of uncoordinated efforts have been made to explain away the differences, yet no clear picture of the relationships between the four populations has emerged. During the >24 hour period on Oct 19-20, 1995 in which a magnetic cloud passed by the magnetosphere the solar wind velocity, magnetic field magnetic magnitude and IMF sector were near constant, while  $B_z$ , the ion density and the ion temperature underwent major changes, for the most part in a steady manner. Ignoring the morphological changes in cusp, boundary and polar rain populations due to changes in  $B_z$ , we compare changes in densities and temperatures to those in the solar wind and relate these to possible entry scenarios.

<sup>1</sup>USAF Phillips Laboratory, Hanscom AFB MA

<sup>2</sup>Boston College, Institute for Scientific Research, Chestnut Hill MA

## **Ion Poleward Boundaries and Convection Reversals during the 18-20 October 1995 Magnetic Cloud Passage**

T. Fehringer<sup>1</sup>, M. S. Gussenhoven<sup>1</sup>, F. Rich<sup>1</sup>, and C. Huang<sup>2</sup>

The polar cap boundary has been defined by a variety of physical conditions: the poleward boundary of discrete aurora, the onset of polar rain, the termination of ion precipitation, and plasma convection reversal, to name the more common ones. Although most theoretical models of the physical processes in the magnetosphere indicate that these boundaries should coincide, in fact, they do not. In a recent statistical study, using data from the DMSP satellites, we found that, on average, the termination of ion precipitation occurred at latitudes 2-3 degrees higher than the plasma convection reversal in the dawn and dusk sectors of the polar cap-auroral region. However, the variation about the average was very large, and in many cases the convection reversal could be at higher latitudes than the ion precipitation boundary. The October 18-20, 1995 passage of a magnetic cloud affords the opportunity to better understand what determines the relationship between the two boundaries since solar wind conditions are near-constant (speed, density, temperature, magnitude of B, and sector) or slowly varying (Bz, from large and negative to large and positive) for the better part of a 24 hour period. We find that even under slowly varying conditions the relationship between the ion poleward boundary and the convection reversal is extremely complex, even though there is an overall trend for both to move to higher latitudes as Bz turns northward. The control of boundary positions by Bz is far greater, in this case, than by Kp.

<sup>1</sup>USAF Phillips Laboratory, Hanscom AFB MA

<sup>2</sup>Boston College, Institute for Scientific Research, Chestnut Hill MA

*Abstract submitted for the IEEE Nuclear and Space Radiation Effects Conference in Palm Springs in July 1996:*

## **Solar Cell Degradation Observed by the Advanced Photovoltaic and Electronics Experiments (APEX) Satellite**

K.P. Ray and D.E. Delorey (Institute for Scientific Research, Boston College, Newton MA 02159)

E.G. Mullen and D.A. Guidice (Phillips Laboratory, Hanscom AFB MA 01731)

D.C. Marvin (The Aerospace Corporation, PO Box 9045, Albuquerque NM 87119)

H.B. Curtis and M.F. Piszczor (NASA Lewis Research Center, Cleveland OH 44135)

This paper presents results from the Photovoltaic Array Space Power Plus Diagnostics (PASP Plus) experiment flown on board the Advanced Photovoltaic and Electronics experiment (APEX) satellite launched on 3 August 1994 into a 2552 km X 363 km orbit with a 70° inclination. Results presented are based on 4576 orbits of data from 3 August 1994 to 11 August 1995. Fifteen solar arrays encompassing a wide range of solar cell materials and manufacturing techniques were flown. Comparisons between flight data and predicted performance based on the NASA AP8MIN proton model and methods described in the JPL Solar Cell Handbook [1] are made.

R.V. Hilmer, R.L. Lambour, R.J. Biasca, M. Tautz, and G.P. Ginet, **PL-GEOSpace: Time Dependent Three-Dimensional Visualization of the Space Environment**, EOS Trans., AGU, 77, S219, 1996

PL-GEOSpace is a master program which allows users to create and rapidly examine in three-dimensions data sets output from a collection of often-used space environment models [Biasca et al., EOS Trans., AGU, 76, S257, 1995]. The recent addition of a dynamic environment module to the PL-GEOSpace code provides that capability of running time-dependent and CPU intensive science models driven by a single coordinated data base including a variety of ground and space based quantities such as Kp, Dst, auroral boundary locations, sunspot number, F10.7 flux, solar wind density and velocity, and the IMF components. We present examples of the time-dependent specification of the unified ionosphere and magnetosphere environments during storm periods as constructed with the use of models recently added to the dynamic environment module of the code, namely (1) the Rice University Magnetospheric Specification Model (MSM) which provides time-dependent electron and ion flux profiles, (2) the Auroral model of Hardy et al. [JGR, 96, 5539, 1991], which supplies statistical representations of electron and ion precipitation in the ionosphere, and (3) the Parameterized Ionosphere Model (PIM) of Daniell et al. [Radio Sci., 30, 1499, 1995] which specifies electron densities in the E and F layers. Future model additions will include particle drift trajectories, solar wind transport, and interplanetary shock propagation. Information on the currently available version of PL-GEOSpace can be found on the USAF Phillips Laboratory homepage (GPS Division) at <http://www.plh.af.mil>.

R.V. Hilmer, G.P. Ginet, and T.E. Cayton, **A Multi-Satellite View of Energetic Electron Flux Increases at L=4-7 Associated with High Speed Solar Wind Streams**, EOS Trans., AGU, 77, F593, 1996

We examine energetic electron flux enhancement events occurring near the equator in the radial range  $L = 4-7$  Re which are associated with high speed solar wind streams during 1995. In the magnetosphere, these events are identified as having geosynchronous fluxes of high energy electrons ( $>2$  MeV) greater than a threshold value of 103 counts/cm<sup>2</sup>/sec/sr/MeV as measure by the Space Environment Monitors on the GOES-7 and GOES-8 satellites. Relevant solar wind conditions are monitored with the help of the WIND satellite. We explore the relationship between the electron enhancement events at  $L=6.6$  Re and similar flux increases of more than an order of magnitude observed in MeV electrons at  $L=4.2$  Re by characterizing the temporal and spatial development of the respective enhancements. We also examine possible correlations involving the degree of electron energization at the two altitudes. In the high L region, additional differential-energy electron data (0.2 to 2.0 MeV) are provided by six Los Alamos geosynchronous satellites distributed in local time and equipped with the Synchronous Orbit Particle Analyzer (SOPA). In the low L region, three GPS Navstar satellites equipped with the Los Alamos electron dosimeter BDD-II (NS-24, NS-28, NS-39) provide data from seven electron channels spanning 0.2 to 5.9 MeV.

M.F. Thomsen, L.A. Weiss, D.J. McComas, G.D. Reeves, and R. Hilmer, **An Observational Test of the Hilmer-Voigt Magnetic Field Model at Geosynchronous Orbit**, EOS Trans, AGU, 77, F593, 1996.

**Abstract.** The Hilmer-Voigt (H-V) magnetic field model is one of the core components of the Rice University Magnetospheric Specification Model (MSM) and its descendant, the Magnetospheric Specification and Forecast Model (MSFM). In this study we test the ability of the Hilmer-Voigt model to reproduce the range of field inclination angles observed at geosynchronous orbit under a wide range of magnetospheric activity. Using magnetic field directions determined from the symmetry axis of electron distributions measured by the Los Alamos magnetospheric plasma analyzers (MPA) on three geosynchronous satellites, we compare the range of observed field directions with the range of directions predicted by the model for those locations. The comparison is done for one month of data at each equinox and solstice.

R.V. Hilmer, G.P. Ginet, and T.E. Cayton, **Requirements for Energetic Electron Flux Enhancements Near  $L = 4.2$ : Relative Geosynchronous Phase Space Density and Geomagnetic Activity**, Geophys. Res Lett., (to be submitted) 1997

We examine the relationship of energetic equatorial electron flux enhancements occurring near  $L = 4.2$  and  $6.6$  which are associated with 12 well defined high speed solar wind streams (HSSWS) detected by the WIND spacecraft during 1995. These events were selected for having high energy ( $>2$  MeV) geosynchronous electron flux levels surpassing  $10^3/\text{cm}^2/\text{sec}/\text{sr}/\text{MeV}$  for periods of greater than a day as measured by GOES 7 and GOES 8. Los Alamos differential-energy electron data from both the Synchronous Orbit Particle Analyzer (SOPA), spanning  $0.2$  to  $2.0$  MeV, and the BDD-II dosimeters aboard GPS Navstar satellites, spanning  $0.2$  to  $3.2$  MeV, illustrate that flux dropouts are typically observed in all energy channels at both equatorial altitudes within the first day of each event. While SOPA at  $L = 6.6$  consistently records post-dropout flux enhancements, GPS dosimeters at  $L = 4.2$  detects equatorial enhancements, for example, in  $1.6$ - $3.2$  MeV electron fluxes in only 9 of 12 events and all are either concurrent (1) with or follow (8) the geosynchronous increases of electrons with similar  $m$  values. We determine that these post-dropout MeV equatorial electron flux enhancements near  $L = 4.2$  occur only while two conditions are concurrently satisfied. First, the phase space density at geosynchronous altitudes must be greater than that at GPS equatorial altitudes, i.e.,  $[f(\text{geo})-f(\text{gps})]>0$  for particles with similar  $m$  values, and second, geomagnetic activity must be elevated such that  $K_p>3$ . With  $[f(\text{geo})-f(\text{gps})]>0$  implying the existence of an outward gradient in phase space density between these altitudes and  $K_p>3$  indicating increased equatorial electron field activity may exist in the same region, we have conditions that might contribute to the inward radial diffusive transport of equatorial electrons and ultimately the observed electron flux enhancements at GPS equatorial altitudes.



**R.V. Hilmer, A Magnetospheric Neutral Sheet-Oriented Coordinate System for MSM and MSFM Applications**, (to be submitted as a Phillips Laboratory Technical Report when code is approved for installation at the USAF 50th Weather Squadron)

We develop a magnetospheric neutral sheet-oriented coordinate system for incorporation into procedures currently used to derive three-dimensional energetic particle flux and magnetic field information from Magnetospheric Specification Model (MSM) simulations. These procedures, i.e., the computer codes MAP3D and FLUX3D, are limited by their reliance on magnetospheric magnetic field configurations which do not account for tilt variations of the Earth's internal dipole field or changes in geomagnetic activity. Consequently, these configurations do not realistically represent a satellite's position relative to the magnetic neutral sheet, which is moving in response to these same quantities. This can result in magnetic field mapping errors as one moves away from the magnetic neutral sheet because magnetic field lines cross it at rapidly greater distances from Earth. Erroneous magnetic field mappings to the MSM simulation region, coincident with the plasma sheet and its imbedded neutral sheet, lead to incorrect particle flux specifications when the dipole tilt angle is large and the magnetic activity index Kp is high. Mapping errors occur in the MAP3D algorithm because satellite locations are provided in GSM coordinates and information about their positions relative to the magnetic neutral sheet is not communicated. To remedy the situation, results from published studies describing the tilt and Kp dependent flexing and warping of the neutral sheet are used to guide development of our new magnetospheric coordinate system. It is suggested that improved MSM particle flux and magnetic field specification can be achieved by translating all position information input to the MAP3D algorithm from GSM coordinates into this neutral sheet-oriented coordinate system.

R.A. Wolf, J.W. Freeman Jr., B.A. Hausman, R.W. Spiro, R.V. Hilmer, and R.L. Lambour, **Modeling Convection Effects in Magnetic Storms**, (accepted for publication in an AGU Monograph based on Chapman Conference on Magnetic Storms, held at JPL, 2/96) 1997

Over the last twenty years, many quantitative models have been developed to represent the idea that the storm-time ring current consists primarily of particles from the plasma sheet that are injected into the inner magnetosphere by strong westward electric fields. These models, which have gradually become more sophisticated and realistic, have achieved rough quantitative agreement with observed ring-current fluxes, but the test are still imprecise. The models are still no sophisticated enough to provide accurate and reliable theoretical estimates of Dst. Controversy still surrounds the question of whether the injection of the storm-time ring current mainly results from induction electric fields associated with magnetospheric substorms or from potential electric fields associated with periods of strong convection. A series of computer experiments has been carried out with the Magnetospheric Specification and Forecast Model in an attempt to illuminate this key question, as well as several other cause-and-effect relationships. The MSFM runs indicate that potential convection electric fields play a far more important role in ring current injection than do substorm-associated induction fields. The computer experiments also demonstrate the importance of fluctuations in the convection field: periods of very strong convection, separated by periods of weak flow, inject particles deeper into the magnetosphere than a long period of moderately strong convection. A run carried out with strong convection limited to one hour - an imitation of a very strong isolated substorm - shows the injection of only a weak ring current. Run results also show reduced populations of ~50 keV ions in regions that are in the shadow of the magnetopause; these depleted regions are particularly prominent when the magnetosphere is highly compressed.

*Poster at 1996 Fall AGU Meeting:*

### **Calculated Radiation Belt Electron Lifetimes Compared to CRRES Observations**

J.M. Albert (Boston College, Newton MA 02159; ph. 617-377-3992; e-mail: albert@sheila.plh.af.mil)

Radiation belt electrons, in the conventional picture, are subject to Coulomb collisions and pitch-angle scattering by turbulent whistler waves (hiss), which limit their lifetimes as trapped particles. Here, updated calculations of these lifetimes are presented, keeping all relevant cyclotron harmonics and using the detailed dispersion relation of Lyons [1974]. These lifetimes are compared to decay times of electron flux enhancements repeatedly observed by CRRES.

### **J.M. Albert, CRRES Observations and Radial Diffusion Theory of Radiation Belt Protons, AGU monograph Monograph vol. 97, "Radiation Belts: Models and Standards"**

The phase space density of high-energy, equatorially mirroring radiation belt protons, as measured by CRRES, is analyzed in terms of radial diffusion. Only the period prior to the magnetic storm of 24 March 1991 is considered. The observed profiles differ drastically from the NASA AP8 models, and also from steady state solutions of the radial diffusion equation, indicating a non-steady configuration. Rates of change of the observed profiles are calculated according to the diffusion equation and compared to the observed time development. Good agreement is obtained for  $L \leq 2.5$  and  $E$  up to about 20 MeV.

### **Comparison of CME Mass and Kinetic Energies Near the Sun and in the Inner Heliosphere**

D.F. Webb (Institute for Space Research, Boston College, Newton Center MA)  
R.A. Howard (Naval Research Laboratory, Washington DC)  
B.V. Jackson (CASS, University of California at San Diego, La Jolla CA)

Published in Solar Wind 8, eds. D. Winterhalter et al., AIP Conf. Ser.382, Woodbury, NY, p. 540, 1996

Masses have now been determined for many CMEs observed in the inner heliosphere by the Helios 1 and 2 zodiacal light photometers. The speed of the brightest material of each CME has also been measured so that, for events having both mass and speed determinations, their kinetic energies can be estimated. We compare the excess masses and kinetic energies of individual CMEs estimated in the inner heliosphere by Helios and near the Sun from observations by the Solwind (1979-1980) and SMM coronagraphs (1980). We also compare the speeds of the same CMEs. We find that the Helios mass and energy estimates are larger by factors of  $\sim 3$  and  $3 - 8$ , respectively, than those derived from the coronagraph data. Possible causes for the mass difference include the extended flow of CME mass through the corona that is not well measured by coronagraphs, and an increase of CME mass with height due to compression of ambient solar wind material. These results provide an important baseline for observations of CMEs from coronagraphs, from the WIND and Ulysses spacecraft and in the near future from SOHO.

## **CMEs as Solar Drivers of Interplanetary and Terrestrial Disturbances**

David F. Webb (Institute for Scientific Research, Boston College, Newton MA 02159)

Published in *Solar Drivers of Interplanetary and Terrestrial Disturbances*, eds. K. S. Balasubramaniam et al., ASP Conf. Ser. 95, p. 208, BookCrafters, San Francisco, 1996

An important new paradigm in solar-terrestrial physics is that coronal mass ejections (CMEs), not solar flares, are the key causal link between solar activity and major interplanetary (IP) particle events and geomagnetic storms. Recent research implies that CMEs drive all large geomagnetic storms, and that fast CMEs produce transient IP shocks which trigger sudden commencements at Earth. Evidence suggests that the CME-related shocks also accelerate the solar energetic particle events associated with major IP disturbances and hazardous effects at Earth. This new viewpoint requires changes in how we prioritize the development of instruments and techniques for forecasting IP disturbances and geomagnetic activity.

## **Geomagnetic Storms and Heliospheric CMEs as Viewed From HELIOS**

David F. Webb (Institute for Scientific Research, Boston College, Newton MA 02159)  
Bernard V. Jackson, Paul Hick (CASS, University of California at San Diego, La Jolla CA 92093)

Published in *Solar Drivers of Interplanetary and Terrestrial Disturbances*, eds. K. S. Balasubramaniam et al., ASP Conf. Ser. 95, p. 167, BookCrafters, San Francisco, 1996

In recent years much progress has been made in understanding the causes of geomagnetic storms. Such storms near solar maximum are now thought to be associated with transient solar activity, especially coronal mass ejections (CMEs) which rate of occurrence tends to track the solar cycle. Most storms occurring during the declining phase of the cycle are associated with fast solar wind arising from coronal holes, but the strongest storms occur during Earth passage of corotating interaction regions which sources are coronal streamer/hole boundaries (Crooker and Cliver, 1994; Lindsay et al., 1995). Since many CMEs involve coronal streamers, it is likely that CMEs are also an important cause of large storms later in the cycle.

## **CMES and Their Relation to Other Disturbances**

David F. Webb (Institute for Scientific Research, Boston College, Newton MA 02159)

Published in *Proc. of the Workshops on Solar Flares and Related Disturbances and on Solar-Terrestrial Predictions-V*, Hiraiso S-T Research Center, CRL, Izozaki, Japan (in press), 1997

Coronal mass ejections (CMEs) are immense structures of plasma and magnetic fields that are expelled from the Sun into the heliosphere. CMEs can cause large geomagnetic storms and the faster CMEs drive transient interplanetary shocks, which in turn accelerate solar energetic particle events, possibly even to GeV energies. This recent understanding has led to an important new paradigm in solar-terrestrial physics that CMEs, not solar flares, are considered a key causal link between solar activity and major interplanetary particle events and geomagnetic storms. At the Sun the onset of CMEs has been associated with both flares and filament eruptions, but most flares and CMEs are independent of each other and

many CMEs cannot be associated with any surface activity. I review what we know about the origins and characteristics of CMEs at the Sun, and some aspects of their manifestation in the inner heliosphere.

### **Large-Scale Structures and Multiple Neutral Lines Associated with Coronal Mass Ejections**

D.F. Webb (Institute for Scientific Research, Boston College, Newton MA)

S.W. Kahler (Geophysics Directorate, Phillips Laboratory, Hanscom AFB MA)

P.S. McIntosh (Heliosynoptics, Inc., Boulder CO)

J.A. Klimchuk (E.O. Hulburt Center for Space Research, Naval Research Laboratory, Washington DC)

Published in J. Geophys. Res. (in press), 1997

We use Yohkoh Soft X-ray Telescope (SXT) images of eruptive events visible against the solar disk to examine the coronal structures and the boundaries of the large-scale magnetic fields considered to be involved in coronal mass ejections (CMEs). From an initial list of about 100 large-scale events, we selected five for detailed study. The transient X-ray structures in these events spanned distances across the solar surface ranging from 35 to >100 heliographic degrees, comparable to the spans of white light CMEs observed at the limb. The widths of the coronal loop arcades spanned two or three neutral lines, or a single, highly convoluted neutral line. The results imply that multipolar magnetic systems are a common configuration of the source fields of many CMEs, contrary to the first-order approximation that CMEs involve the eruption of simple, bipolar structures.

### **The Solar Mass Ejection Imager**

B.V. Jackson, A. Buffington, P.L. Hick (Center for Astrophysics and Space Sciences, UCSD, La Jolla CA 92093)

S.W. Kahler (Phillips Laboratory/GPSG, Hanscom AFB MA 01731)

S.L. Keil, R.C. Altrock (Phillips Laboratory/GPSS, National Solar Observatory, Sacramento Peak, Sunspot NM 88349)

G. Simnett (Space Research Group, University of Birmingham, Birmingham, UK)

D.F. Webb (ISR, Boston College, Newton MA 02159)

Published in Proc. of Small Mission Opportunities and the Scientific Community Workshop, W. Pecorella and R. Mura, eds., Collefero, Italy, in press, 1996

We are designing a Solar Mass Ejection Imager (SMEI) capable of observing Thomson-scattered signals from transient density features in the heliosphere from a spacecraft situated near 1 AU. The imager is designed to trace these features, which include coronal mass ejections, corotating structures and shock waves, to elongations greater than 90° from the Sun. The instrument may be regarded as a progeny of the heliospheric imaging capability shown possible by the zodiacal light photometers of the HELIOS spacecraft. The instrument we are designing would make more effective use of *in situ* solar wind data from spacecraft in the vicinity of the imager by extending their observations to the surrounding environment. An imager at Earth could allow up to three days warning of the arrival of a mass ejection from the Sun.

*Abstracts of presentations at the Fall AGU meeting held in San Francisco, 15-19 December 1996:*

### **X-ray Signatures of CMEs Observed in White Light**

D.F. Webb (ISR, Boston College, Newton Center MA, 02159)  
H.S. Hudson (SPRC, 4720 Calle Desecada, Tucson AZ 85718)  
R.A. Howard (NRL, Washington DC 20375)

Although CME models often invoke the opening of previously closed magnetic fields in the lower corona, identifying consistent signatures of CME onset near the surface has proven elusive. We summarize results from several recent studies using Yohkoh/SXT observations of X-ray transient structures considered possible onset signatures of CMEs. One study is of large-scale, long-duration X-ray arcade events which exhibit dimming, or depletion of the corona. In addition we are examining the SXT data during periods when white light CMEs were observed from the HAO Mauna Loa Observatory or the NRL LASCO spaceborne coronagraphs on SOHO. We searched for transient X-ray structures, involving brightenings and motion, occurring during time intervals and limb locations consistent with the onset times of the MLO and LASCO CMEs. Preliminary results suggest that the typical X-ray structure associated with CME onsets is a loop-like expansion associated with a flaring active region. However, many of the LASCO CMEs do not have clear X-ray signatures; one interpretation is that their detectability near solar minimum is poor because of the weak coronal emission.

### **Heliospheric Imaging Using the Helios Photometers and Thomson Scattering Techniques**

D.F. Webb (ISR, Boston College, Newton MA 02159)  
B.V. Jackson (UCSD/CASS, 9500 Gilman Dr., La Jolla CA 92093)

Over the last ten years, we have utilized data from the zodiacal light photometers on the twin Helios spacecraft to image structures in the inner heliosphere. Although the zodiacal dust cloud dominated the signal observed by the instrument, its invariant signal could be removed from the data by using a model for the zodiacal light brightness and a suitable temporal filter. The remaining residual variations contain electron-scattered components of sunlight which map a variety of heliospheric structures. These include solar mass ejections observed in the inner heliosphere, structures such as streamers which corotate with the Sun, and density enhancements associated with shock waves. The Helios photometers viewed the sky globally around the spacecraft, even tracing the outward motion of material past the spacecraft into the anti-solar hemisphere. Some of these structures have been imaged as they traveled along the Sun-Earth line, providing tests of our ability to forecast their arrival and effects at Earth. The three-dimensional views of dense structures in the outward-flowing solar wind can be deconvolved and represented in tomographic reconstructions.

## **Coronal Mass Ejections and Metric Type II Bursts**

E.W. Cliver (PL/GPSG, Hanscom AFB MA 01731-3010)  
D.F. Webb (ISR, Boston College, Newton MA 02159-1164)  
R.A. Howard (NRL, Code 4170, Washington DC 20375)

The origin of the coronal shock waves that manifest themselves as slow drift (metric type II) bursts is controversial. The extreme viewpoints are either that: (1) all type II bursts are blast waves caused by the sudden release of energy during a solar flare, or that (2) all type IIs are piston-driven by fast coronal mass ejections (CMEs). Of course, it is possible that type IIs may be caused by both mechanisms. The question then becomes one of degree; which mechanism is dominant? In this study, we review the arguments for both viewpoints and present a comprehensive comparison of type II and CME data, using Solwind coronagraph observations for the 1979-1985 period.

*Abstracts of presentations at IAU Colloquium 167 to be held in Aussois, France, 28 April-5 May 1997:*

## **CMEs and Prominences and Their Evolution Over the Solar Cycle (Invited)**

David F. Webb (ISR, Boston College, Chestnut Hill MA 02167-3862, USA)

CMEs are an important aspect of coronal and interplanetary dynamics. They cause large geomagnetic storms and can drive transient interplanetary shocks, which in turn are the source of energetic particle events. However, our knowledge of the origins and early development of CMEs at the Sun is limited. CMEs are most frequently associated with erupting prominences and long-enduring soft X-ray arcades, but sometimes with no observed surface activity. I will review some of the well-determined coronal properties of CMEs and what we know about their source regions, with emphasis on the characteristics of the associated filaments/prominences and helmet streamers. One of these characteristics is that many CMEs seem to arise from multipolar magnetic structures with multiple or kinked inversion lines. Finally, I will discuss the solar-cycle dependences of these structures, including the role that erupting prominences and CMEs may play in the ejection of magnetic flux and helicity that are built up during the solar cycle.

## **Sudden Disappearances of Polar Crown Filaments as Sources of High Latitude CMEs**

E.W. Cliver (Air Force Research Laboratory, Hanscom AFB MA 01731-3010)  
D.F. Webb (Institute for Scientific Research, Boston College, Chestnut Hill MA 02167 USA)

We examine the possible sources of the high-latitude ( $>45$  degrees) CMEs that are a characteristic feature of solar maximum. In particular, we address the relative importance of sudden disappearances of polar crown filaments and of the filaments lying equatorward of the polar crown, that will form the polar crown for the subsequent cycle, as sources of such CMEs. Projection effects, backside sources, and CMEs that originate in the eruption of magnetic arcades which lack tracers are taken into account. Data sources include neutral line maps, the Meudon and Wright catalogs of filament disappearances, and CME observations from Solwind and SMM.